Vol. 156: 1–16, 1997 | MARINE ECOLOGY PROGRESS SERIES
Mar Ecol Prog Ser | Published September 25

Carbonate dynamics of the coral reef system at Bora Bay, Miyako Island

Steven Kraines[1,*], Yoshimi Suzuki[2], Tamotsu Omori[3], Kiminori Shitashima[4], Satsuki Kanahara[5], Hiroshi Komiyama[1]

[1]Department of Chemical Systems Engineering, University of Tokyo, 7-3-1 Hongo, Bunkyo-ku, Tokyo 113, Japan
[2]Department of Earth Science, Shizuoka University, Shizuoka, Japan
[3]Department of Analytical Chemistry, University of the Ryukyus, Naha, Okinawa, Japan
[4]Central Research Institute for the Electric Power Industry, Abiko, Chiba, Japan
[5]Graduate School of Environmental Earth Science, Hokkaido University, Hokkaido, Japan

ABSTRACT: Direct measurements of total inorganic carbon, total alkalinity and pH were obtained together with salinity, temperature and current velocities in a coral reef at Bora Bay, Miyako Island in the Ryukyu Islands in October 1993, March 1994 and July 1994. The 3 parameters of the carbonate system showed good internal consistency using carbonate acid dissociation coefficients from the literature, although the total alkalinity values observed in July were lower than the calculated values. Comparison of calculated values of the fugacity of CO_2 in the coral reef waters and in the outer oceanic waters suggested that, particularly where water flows out of the lagoon and back to the ocean, biological activity within the reef-lagoon system may be releasing CO_2 to the reef waters. However, a more careful consideration of biological inorganic and organic carbon production showed that the reef flat was a strong sink for aqueous CO_2 in July. The lagoon, on the other hand, appears to be a slight source of CO_2 in October and March.

KEY WORDS: Coral reef · Coral metabolism · Calcification Total inorganic carbon · Carbonate cycle

INTRODUCTION

The complexity of coral reefs together with the naturally high rate of gross organic production occurring in the reef ecosystem (Lewis 1977) has attracted much interest in the biogeochemical carbon cycle of coral reefs (Crossland et al. 1991, Kinsey & Hopley 1991, Smith & Veeh 1989, Gattuso et al. 1993, Suzuki et al. 1995). Towards this end, a large body of data has been assembled by coral reef researchers (Kinsey 1985). The biological communities of coral reefs influence the carbonate chemistry of the reef waters through the interaction of 2 processes, organic production and calcification. This situation is further complicated by the exchange of CO_2 between the air-sea interface. In addition, coral reefs, like other coastal marine ecosystems, are highly open to the surrounding ocean. Therefore, the advective transport of materials by sea water circulating through the reef system plays an important role in the biogeochemical cycle of carbon within a coral reef (Smith 1984, Hamner & Wolanski 1988). In a series of papers, Atkinson & Bilger presented evidence that the physical flow of water plays an important role in facilitating the transport of essential nutrients from the bulk water column to the coral organisms (Atkinson et al. 1992, Bilger et al. 1995).

In order to understand the carbon cycle of coral reefs, we must develop analytical tools that enable us to assess the role of this advection together with the role of biological processes on the carbonate chemistry of the coral reef ecosystem. These analytical tools should enable us to obtain more information regarding the underlying mechanisms of the carbon cycle from data obtained from sampling efforts. Simple and elegant conceptual models are expected to play an

*E-mail: kraines@komiyama.t.u-tokyo.ac.jp

important role in developing these tools (Kraines et al. 1996).

Here, we examine the inorganic carbon cycle in a small coral reef lagoon at Miyako Island, the Ryukyu Islands, using measurements of 3 of the carbonate parameters: pH, total alkalinity (A_T) and total inorganic carbon (TIC). TIC measurements were carried out using a modification of the coulometric method described by Johnson et al. (1987), and offer some of the first high precision TIC measurements in a coral reef. When combined with standard pH and A_T measurements, we can examine the internal consistency of our measurements by cross-checking each parameter since only 2 parameters are required to describe the carbonate system (Dickson & Goyet 1994).

We also use the combinations of pH-TIC, pH-A_T and TIC-A_T to calculate the fugacity of carbon dioxide, fCO_2, in the reef waters. Note that it is correct to use the term 'fugacity' here rather than 'partial pressure' since fugacity accounts for the deviation of the behavior of the gas from the ideal gas law (Dickson & Goyet 1994). By comparison with oceanic fCO_2, we evaluate the spatial and seasonal tendencies for CO_2 fluxes to and from the reef ecosystem. Finally, we develop a simple biophysical flow model for the reef system to estimate rates of organic and inorganic production at Bora Bay as functions of solar irradiance.

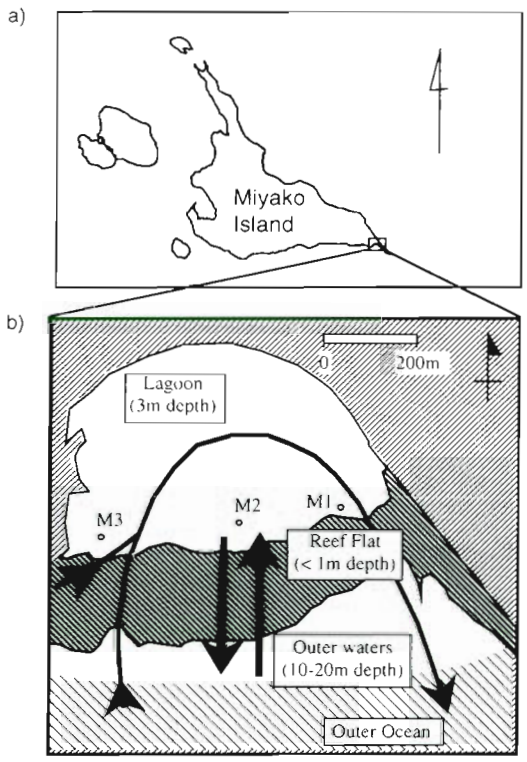

Fig. 1 (a) Study site at Bora Bay, Miyako Island. (b) Detail of reef and lagoon at Bora Bay with arrows showing the general flow pattern described by Kraines et al. (1996). The main observation stations, M1, M2 and M3, are also shown

MATERIALS AND METHODS

We conducted field surveys at the coral reef and lagoon at Bora Bay on October 13 to 15, 1993, March 28 and 29, 1994, and July 22 to 25, 1994.

Study area. The bay is located at the south east tip of Miyako Island in the Ryukyu Island Chain south of Japan at 24° 45' N, 125° 20' E (Fig. 1a). The lagoon/reef system along with the 3 observation points—M1, M2 and M3—are shown in Fig. 1b. The lagoon is parabolic with an area of about 0.25 km^2 and an average depth of 3 m. The reef flat forms a nearly complete boundary between the ocean and the lagoon with an area of about 0.1 km^2. The depth range over the reefflat is −0.2 to 1.3 m during the spring tides, thus the lagoon becomes closed to the ocean at the low spring tide. Observation stations M1 and M3 were chosen to represent the regions of the lagoon where water exits to and enters from the reef flat. M2 was positioned between M1 and M3, just inside the central part of the reef flat. The stations were positioned within the lagoon in order to ensure sufficient depth to allow reliable operation of the observation meters.

Biological community. The biological community of Bora Bay has been described briefly by Kraines et al. (1996). In addition, a detailed description of the percent coverage of coral and some species of algae has been given by Zimmerman et al. (1993). The coral reef and lagoon at Bora Bay is characterized by a wide diversity of marine flora and fauna typical of coral reefs in the western Pacific. Algae is dominant in the lagoon (10 to 40% of total coverage), and coral is dominant on the reef flat.

Sample collection. We collected water samples for analysis of pH, A_T and TIC using a Niskin water sampler during each of the 3 surveys. In October 1993, we sampled every 3 h during the entire day at M1 and during the daytime only at M3 for 2½ d. In March 1994, we sampled at M1 and M2 every 1 to 3 h continuously for 36 h. In July 1994, we sampled at M3 every 2 h for 3 d. For pH and TIC, 1 measurement was made for each time and location. A_T measurements were made twice from a single sample taken for each time and location. In addition to this standard sampling procedure, replicate samples were taken on occasion during all 3 field surveys to assess sampling error as described below.

For pH and A_T sampling, we used acid washed polyethylene bottles. For TIC samples we used 125 ml acid washed glass bottles capped with non air permeable butyl rubber stoppers. The sample bottles were filled

completely, and both pH and TIC samples were allowed to overflow 1 complete volume with sea water from the Niskin bottle in order to minimize gas exchange of the sample water. We added 50 µl of $HgCl_2$ (50% saturated solution) to the TIC samples as recommended by Dickson & Goyet (1994). The bottles were then sealed with the stoppers and alumiseals. A minimal head space of less than 3 ml air was deemed necessary to prevent bottles from cracking during the clamping process and subsequent thermal expansion for the samples taken in October 1993 and March 1994. We calculated the theoretical loss or gain of TIC to a 3 ml head space. For the highest fCO_2 observed (about 680 ppm) less than 0.02% of the carbon is lost, and less than 0.01% is gained for the lowest observed fCO_2 (about 200 ppm). This problem was corrected in the subsequent sampling by cooling samples in coldwater immediately after sealing them to avoid thermal expansion. The TIC samples were then shipped to Tokyo for analysis as described below.

pH and total alkalinity analysis. pH was measured using a Radiometer pHM95 pH/Ion Meter equipped with a Radiometer GK2401C combined glass electrode. The electrode was calibrated against U.S. National Bureau of Standards (NBS) buffers: pH 7.00 and pH 4.01 (Golden Buffer). Measurements were carried out in a closed, glass cell in a constant temperature water bath maintained at 25°C. After calibration with the NBS buffers and prior to sample measurement, the electrode was placed in a solution of 0.7 M KCl for 15 min to acclimate the electrode to the saline environment. From 5 replicate samples of surface water from the central lagoon, we obtained a precision for the pH analysis of ±0.0007 (1 SD).

Alkalinity was determined using the Gran Plot method. A 50 ml sample for determination of total alkalinity was filtered on a 0.45 µm membrane filter and titrated with a Radiometer TIM90 titration manager equipped with an ABU91 autoburette. Titration was carried out in the constant temperature bath at 25°C using a solution of 0.1 M HCl with 0.7 M KCl added to simulate the ionic strength of sea water. Measurements of A_T were carried out in duplicate. The alkalinity titration system was calibrated with a solution of 1000 µM Na_2CO_3 and 0.7 M KCl. The precision of this method of A_T determination from repeated measurement of filtered sea water was calculated to be ±2 µmol l^{-1} (1 SD).

TIC analysis. We have employed the coulometric technique for TIC analysis described by Johnson et al. (1987) to provide high precision and high accuracy measurements of TIC in oceanic waters. Briefly, the method involves stripping a sea water sample of its CO_2 content by acidifying the sample and running a stream of CO_2 free carrier gas through to carry the CO_2 to the coulometric detector.

We used a modified version of the apparatus described by Johnson et al. (1987) for stripping CO_2 from the samples, as shown in Fig. 2. Air is pumped through a KOH trap to remove CO_2. That CO_2 free air is used as the carrier gas which forces sample water into a pipette with a precisely known volume (30 ml). After valve switching, the precise volume of sample water is forced into the reaction vessel. As recommended by Johnson et al. (1987), we add phosphoric acid to the reaction vessel which converts all the inorganic carbon in the sample to CO_2. About 10 min was sufficient for complete stripping of inorganic carbon in the samples using the present system, but we continued the process an extra 5 min. The carrier gas is then used to transport CO_2 from the sample through a $AgNO_3$ trap

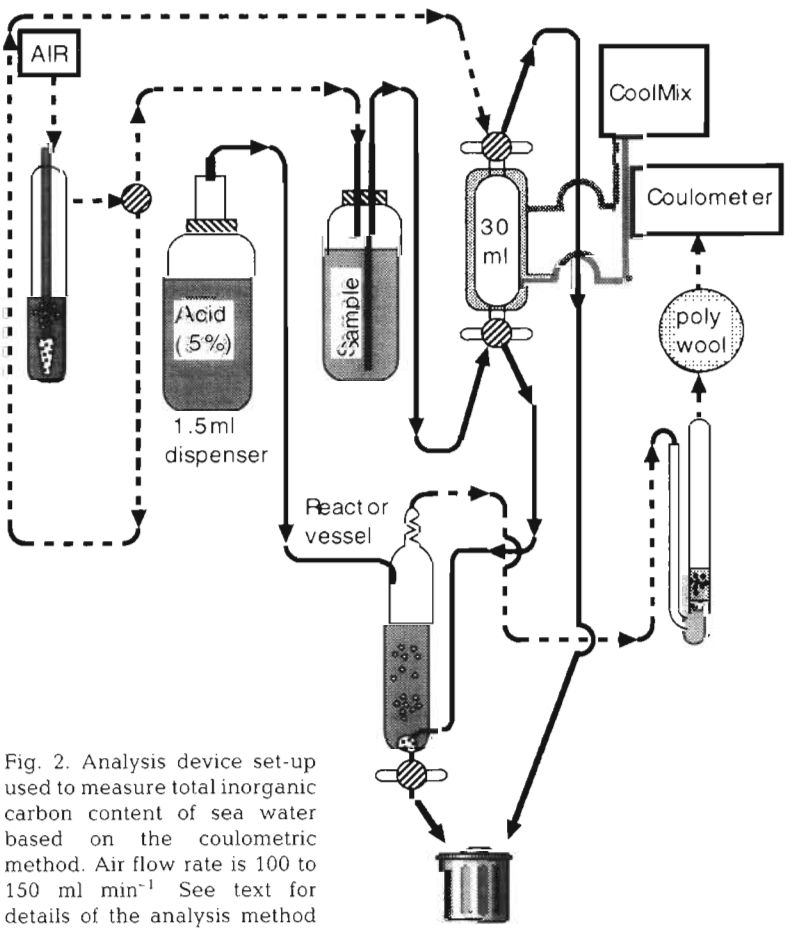

Fig. 2. Analysis device set-up used to measure total inorganic carbon content of sea water based on the coulometric method. Air flow rate is 100 to 150 ml min^{-1} See text for details of the analysis method

which removes chlorine and bromine and a polywool trap to remove water vapor. The gas then enters the coulometer cell where the CO_2 content is analyzed.

The main difference between our system and that employed by other workers is the simplified, manual line system (Fig. 2). This appears to improve response stability, resulting in a near zero background response. That is to say, after 10 min of bubbling the acidified sample, no further response was given by the coulometer. We have also employed a Hirobe trap which, together with the polywool trap, appears to effectively remove water vapor from the carrier gas without added complexity of dehumidifiers. Finally, the narrow line diameter in our system (1.0 mm) appears to decrease memory of previous samples (a problem we had observed previously) as well as allowing a faster time to zero response, i.e. 10 min.

We used a series of 5 liquid phase standards prepared from precisely measured quantities of Na_2CO_3 (>99.999% pure grade) and freshly deionized water to establish a calibration curve. We also used substandards prepared from a tank of well-mixed offshore surface sea water, filtered and poisoned in the same way as described above, to determine the precision of our instrument. From 19 substandard measurements, the precision was determined to be 1.8 µmol l^{-1} (1 SD). Accuracy was investigated by analyzing certified reference materials provided by Andrew Dickson (see Dickson & Goyet 1994). From 2 series of measurements, we calculated mean TIC concentrations within 2 and 3 µmol l^{-1} of Dickson's values. Finally, we determined the precision of the overall TIC sampling and analysis process by measuring replicate samples taken from the lagoon during all 3 of the surveys. The calculated precision was 2 µmol l^{-1} (1 SD calculated from the variation within a group).

We carried out a time delay test in order to test the stability of samples prepared as described above by analyzing samples prepared from the same sampling 3 d, 2 wk and 1 mo after sampling. No drift trend was observed. We concluded that the $HgCl_2$ poisoning was adequate to stabilize the TIC content of the samples.

Light measurements. We measured total irradiance during each of the surveys using a Robichi type irradiance meter placed on the roof of the laboratory located near the survey site. We converted total irradiance to photosynthetically active radiation (PAR) by assuming that 50%of the total irradiance is photosynthetically active (Kirk 1983).

Salinity and current measurements. Salinity and current measurements were obtained using Sanyo Sokki electroconductivity meters (MWQ-III) and Alec Electronics electromagnetic current meters (ACM-8M), respectively, as described in Kraines et al. (1996).

RESULTS

Observed water flow at Bora Bay

The flow meter at M1 showed a primarily outward directed flow (Fig. 3a), and the flow at M3 was directed into the lagoon (Fig. 3b). The flow measured at the center of the lagoon shows a weak longshore current in the lagoon from west to east. Thus the flow at Bora Bay is characterized by a wave forced flow of water over the reef flat and into the lagoon over the western half of the reef flat, longshore current flow through the lagoon, and subsequent draining of the reef flat through a relatively narrow passage in the reef on the east side of M1.

Solar irradiance

All 3 survey periods were characterized by clear weather conditions resulting in nearly perfect sinusoidal solar irradiance profiles such as the one shown in Fig. 3 for the October survey. In October, the maximum light intensity was 1200 µmol photons m^{-2} s^{-1} and the day length was 13.5 h (measured from 30 min before sunrise to 30 min after sunset, corresponding approximately to civil twilight at dawn and dusk, respectively). In March, the maximum light intensity was 2100 µmol photons m^{-2} s^{-1} and the day length was 13.5 h. In July, the maximum light intensity was 2200 µmol photons m^{-2} s^{-1} and the day length was 14 h.

Measured pH, TIC and A_T

The diurnal rise and fall is clearly apparent in the TIC, A_T and pH profiles where 24 h sampling was carried out, for example at station M1 in October as shown in Fig. 3a. We observed outer ocean concentrations of TIC and A_T to be relatively constant in comparison to the lagoon. In October 1993 the standard deviation of 3 oceanic samples taken from around the southeast of Miyako Island was 16.5 µmol l^{-1}. In March 1994, the standard deviation of 16 oceanic samples was 5.9 µmol l^{-1}. In June 1994, the standard deviation of 6 oceanic samples was 11.7 µmol l^{-1}. Of course, the precision of these estimates of the standard deviations will be influenced by sample size. However, the values themselves, which are independent of sample size, are almost an order of magnitude smaller than the range of the diel TIC changes of over 100 µmol l^{-1}. Therefore, the large amplitude of oscillation that we observed in the lagoon is clearly caused by processes occurring within the reef system.

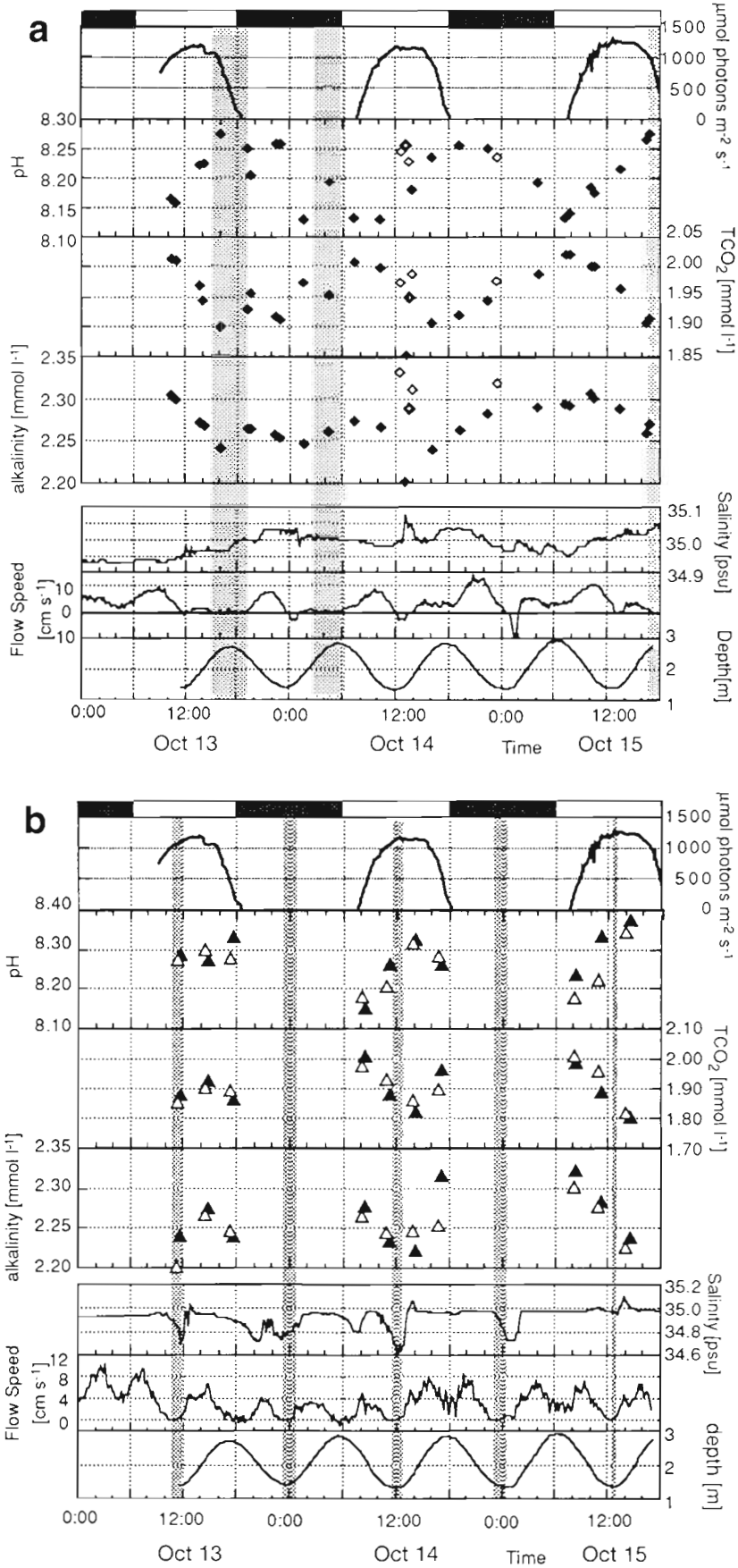

Fig. 3. Observed measurements of light, pH, TIC and total alkalinity from October 1993. Continuous profiles of salinity (psu), flow speed, and depth (m) are also shown. Light is converted from measurements of irradiance assuming that PAR constitutes 50% of total irradiance. Flow speed is directional with positive values showing the velocity in the direction of the arrows in Fig. 1b. (a) Station M1 (◆) and offshore (◇). All line plots show data from station M1. (b) Stations M3 (▲) and M2 (△). All line plots show data from station M3. Shaded regions indicate periods when flow speed is close to zero. See text for detailed explanation

Calculated TIC and carbonate alkalinity (A_C)

In order to investigate the internal consistency of the TIC and A_T measurements, we calculate A_C from observed values of pH and TIC, and TIC from observed pH and A_T, for the times when all data were available. As our values of pH were measured using the NBS scale, we use the formulations of salinity and temperature dependence of the carbonate equilibrium constants, K_1 and K_2, proposed by Mehrbach et al. (1973). Equations for the calculation of the dissociation constant of water K_w, sea water density, and the CO_2 gas equilibrium constant were taken from Dickson & Goyet (1994).

In order to compare the calculated A_C with the observed A_T, we convert the observed A_T to A_C by subtracting the concentrations of borate, OH^- and H^+. Total borate is calculated from the total concentration of boron species times the borate dissociation coefficient given by Johansson & Wedborg (1982) where total boron is estimated as salinity multiplied by a proportionality constant (Millero 1995). Since we need a value for pH to calculate the borate ion concentration from total boron, we use the iterative method described by Ben-Yaakov (1970) to calculate the value of pH which gives a balanced hydrogen ion budget in terms of TIC and A_T.

We use the method of least squares to find the linear regression between observed and calculated TIC and A_C (Fig. 4). Since both the dependent and independent values here have errors from a strict statistics point of view, analysis based on the functional relationship should be applied. However, the error of the observed values (about 0.1%, as shown previously) is much less than the error in the calculated values, which incorporate both the measurement errors and errors in the calculation of the carbonate system. Therefore, the error in the independent variable can be neglected, and the use of the method of least squares is justified.

Theoretically, the relationship between calculated and observed values should be one-to-one and should pass through the origin. We calculated the significance of the *y*-intercept values given by the regression. Using a 95% confidence interval, we determined that the *y*-intercepts were indistinguishable from zero for all data sets except the July data set. Consequently, we have given the equations and R^2 values for linear regressions forced through the origin for the October and March data sets, but for the July data set we give the equations of standard linear regressions not forced through the origin (Fig. 4).

The calculated values correlate well with the observed values, although the calculated TIC are slightly lower than the observed in October and March while the reverse is observed between the calculated and observed A_C. However, the calculated TIC in July is significantly higher than the observed values and the reverse is evident for A_C. We do not have an explanation for this discrepancy at this time. However, as the analysis of pH and A_T is highly sensitive to temperature, it is possible that this offset is due to a slight deviation of the measured temperature from 25°C. A shift of a couple of degrees could account for the shift of the regression line.

Calculated fCO_2

We can calculate fCO_2 from any combination of A_C, TIC and pH by using the carbonate equilibrium constants which are given as a function of temperature and salinity. Also, by using all 3 measured quantities, we can calculate fCO_2 using just 1 of the carbonate equilibrium constants (equations used for these calculations are given in Dickson & Goyet 1994).

The results of calculations of fCO_2 from the 4 combinations of carbonate parameters described above are plotted in Fig. 5. As our sampling precision is best for TIC and pH, we have plotted the percent difference between the fCO_2 calculated from TIC and pH and the values calculated from the other 3 methods. It is readily apparent that while the fCO_2 values calculated from the A_T-pH pair and from all 3 parameters differ from the TIC-pH value by at most 3% in the October and March data sets and 5% in July, the values calculated from A_T and TIC differ by as much as 13% in October, 26% in March and 33% in July.

DISCUSSION

Role of tidal flow on the TIC and A_T profiles

Kraines (1995) showed that the tidal circulation pattern at Bora Bay has a strong influence on the concentration signals of dissolved oxygen observed at M3. Periods where flow speeds at M3 are near zero correspond to the spring low tide when the reef flat emerges and isolates the lagoon from the outer ocean (Fig. 3). During these periods strong changes in salinity occur at M3 (Fig. 3b). Kraines (1995) hypothesized that the sharp drops in salinity are caused by ground water entering the lagoon from the shore, a signal that is usually masked by the dominate oceanic inflow. Following the drop, a small peak is occasionally visible in the daytime profiles. Kraines (1995) ascribed this peak to the ponding of water over the reef flat during the low tide. He showed that since the water is trapped at a very shallow depth, evaporation is able to increase the salinity significantly. When the next tidal flow begins, this highly concentrated water is swept into the lagoon, carrying the high salinity signal to the M3 observation point.

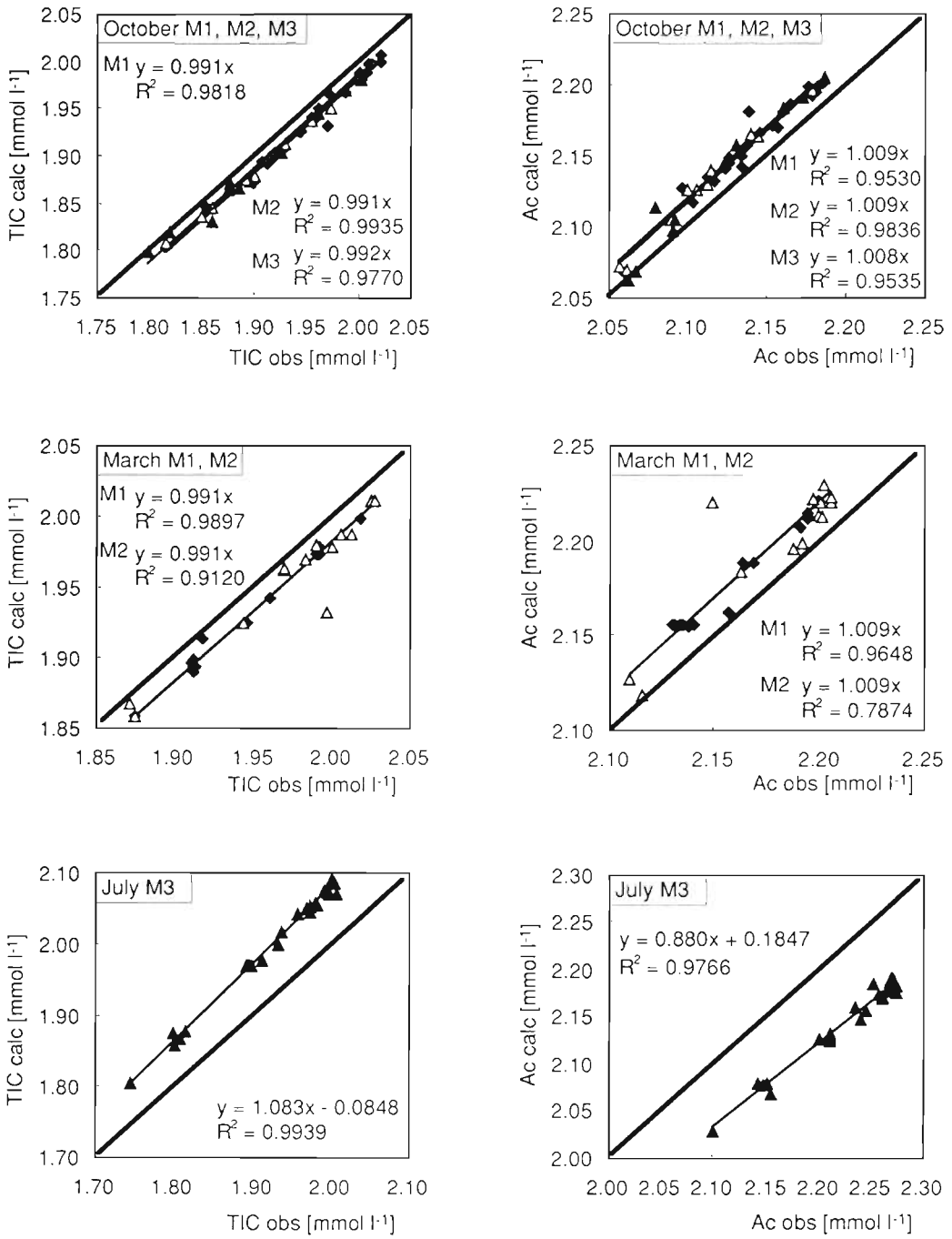

Fig. 4. Correlations between observed and calculated values of TIC and A_T for all data from stations M1, M2 and M3 inside the lagoon. Linear fits and R^2 values are also shown. Linear regressions for the October and March data sets were forced through the origin as described in text. Thick line shows theoretical one-to-one relationship

The same theory was used to explain sharp peaks and dips in dissolved oxygen (DO) observed at M3 (Kraines et al. 1996). In water trapped over the reef flat during the low tide, DO is strongly modified by the biological community on the reef, being increased during the day by photosynthesis and decreased at night by respiration. The flood tide carries this modified water to the M3 observation point resulting in peaks during the day and dips at night.

The reverse pattern appears in the TIC and A_T profiles, with the lowest values of TIC and A_T occurring immediately after the zero flow periods during the daytime (Fig. 3b). TIC and A_T are reduced through photosynthesis and calcification during the day and

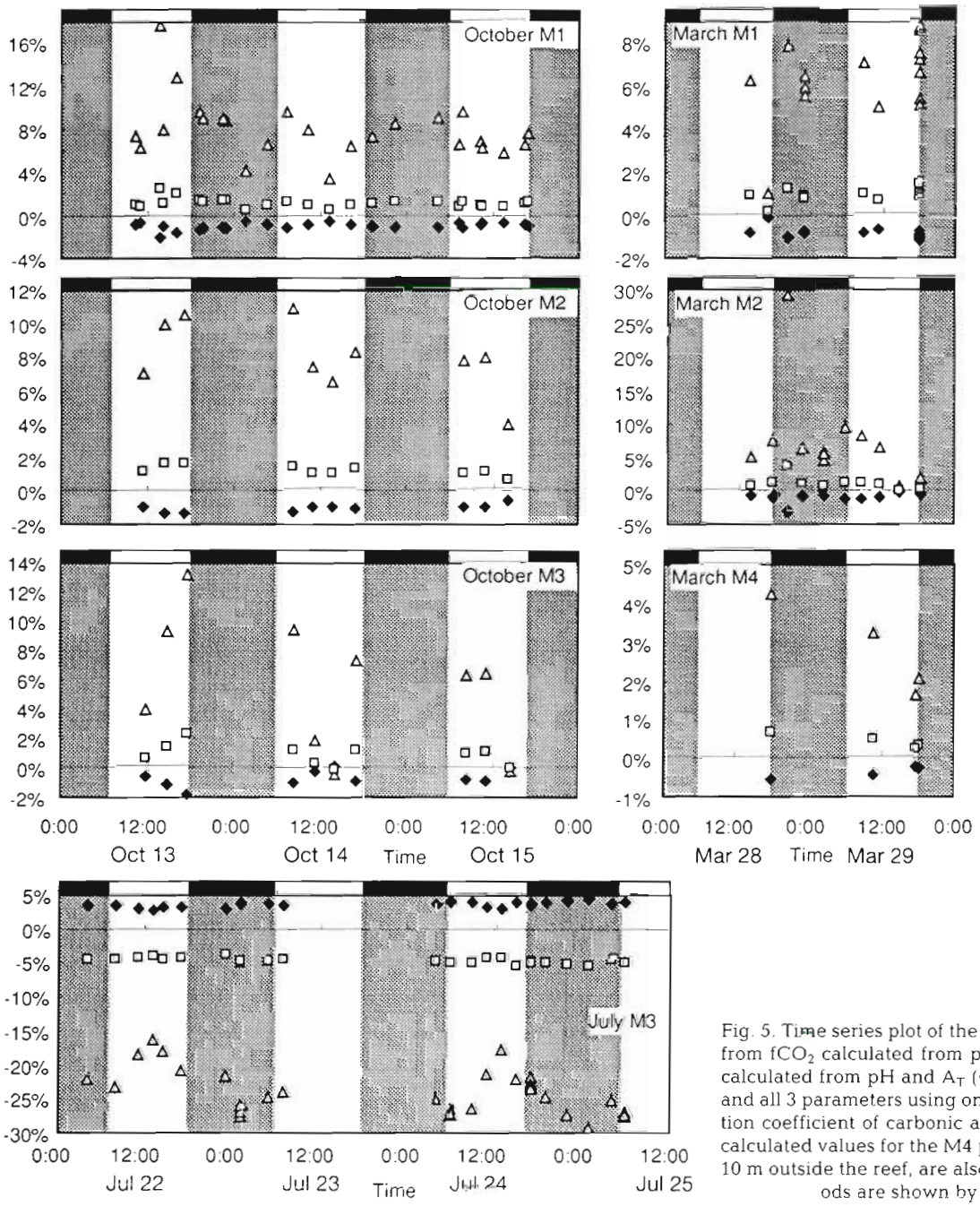

Fig. 5. Time series plot of the percent differences from fCO_2 calculated from pH and TIC of fCO_2 calculated from pH and A_T (◆), TIC and A_T (△), and all 3 parameters using only the first dissociation coefficient of carbonic acid (□). For March, calculated values for the M4 point, located about 10 m outside the reef, are also shown. Dark periods are shown by shading

increased by respiration and dissolution at night, so they show the opposite behavior of DO. At M1, the changes in TIC and A_T are more smooth, and peaks in the profiles are not observed (Fig. 3a). This is in agreement with the observation that flow is directed from the lagoon to the reef flat so the depleted reef flat waters are not carried to M1. Instead, the concentration changes at M1 are caused mainly by the diurnal variation of organic and inorganic production in the lagoon.

Internal consistency of the carbonate system

We obtained good consistency of calculated fCO_2 for all sets of parameters except for the TIC-A_T pair. Ikeda et al. (1995) measured all 4 carbonate parameters in a closed laboratory chamber with and without coral reef organisms. In the case with no living organisms, they obtained generally good thermodynamic consistency in response to additions of acid and base between pH, A_T and TIC. However, they

showed that the propagated errors for fCO_2 measurement were highest when TIC and A_T were used as calculating parameters. Millero et al. (1993) also concluded that, given the precisions and accuracies of the various analytical techniques currently available to determine the parameters of the carbonate cycle, the error in calculating fCO_2 in terms of measured A_T and TIC is 6 times larger than if pH is used with either A_T or TIC. These findings agree with our observation of the divergence of fCO_2 values calculated from TIC and A_T.

Exchange of inorganic carbon across the air-sea interface

The physiochemical process of gas transfer across the air-sea interface to the site of metabolism affects the carbon dynamics in coral reefs since CO_2 can diffuse across that interface.

$$CO_2(aq)^* \rightleftarrows CO_2(g) \quad (1)$$

Here $CO_2(aq)^*$ is defined as the sum of the concentrations of dissolved CO_2 and H_2CO_3. Under typical oceanic surface water conditions of pH and temperature, $CO_2(aq)^*$ forms less than 1% of TIC, on the order of 10 to 20 µmol l^{-1}. The rate of gas exchange across a liquid-gas interface is usually approximated as the concentration gradient across the interface times a wind and temperature dependent gas exchange factor, i.e. the stagnant film model (Broecker & Peng 1974, Smith 1985). Only about 1% of an increase in TIC occurs as an increase in $CO_2(aq)^*$, the gas exchangeable portion. The remaining 99% of the added CO_2 reacts with water to form HCO_3^- and CO_3^{2-}, which do not exchange across the air-sea interface. Therefore, the instantaneous rate of gas evasion for a given increase of TIC might be expected to be about 100 times slower than the corresponding evasion rate of a non-reactive gas.

In fact, since HCO_3^- is converted simultaneously to $CO_2(aq)^*$, the relative change in $CO_2(aq)^*$ is actually much larger than the relative change in the overall TIC. This phenomenon is described by the Revelle factor, defined as the ratio of the change in $CO_2(aq)^*$ over the total quantity of $CO_2(aq)^*$ and the change in TIC over the total quantity of TIC:

$$\text{Revelle factor} = [\Delta CO_2(aq)^*/CO_2(aq)^*]/(\Delta TIC/TIC) \quad (2)$$

This value ranges from 8 to 14 in the world's oceans (Broecker & Peng 1982). We can rewrite the Revelle factor as $[\Delta CO_2(aq)^*/\Delta TIC] \times [TIC/CO_2(aq)^*]$. Since $TIC/CO_2(aq)^*$ is approximately 100 (from above), for a Revelle factor of 10 a gain of 100 mol of TIC results in the loss of not 1 but 10 mol of $CO_2(aq)^*$. Thus we would expect gas exchange for TIC to be only about 7 to 12 times slower than a non-reactive gas.

To examine the difference of equilibration times between dissociating gases such as CO_2 and non-dissociating gases such as O_2, we apply some typical numbers from Bora Bay to the equations described above. We use a water depth of 3 m, the approximate depth at Bora Bay. For a pH of 8.25, a temperature of 27°C and a salinity of 34.8 psu, a TIC of 1900 µmol l^{-1} gives us a $CO_2(aq)^*$ concentration of 9.5 µmol l^{-1} or about 0.5% of the TIC concentration. If we increase TIC to 2000 µmol l^{-1} while holding A_T constant, the concentration of $CO_2(aq)^*$ increases 5.7 µmol l^{-1} to a total concentration of 15.2 µ mol l^{-1}. The resulting initial rate of gas exchange, using the wind dependent formulation of the gas exchange coefficient proposed by Wanninkoft (1992) and a typical wind speed of 5 m s^{-1}, is less than 20 mmol m^{-2} d^{-1}. If we calculate the change in $CO_2(aq)^*$ as the system re-equilibriates, holding A_T, temperature and salinity constant, we find that it takes almost 240 h, or 10 d, to reduce the fCO_2 difference between the water and the atmosphere by half. However, the half time of the system to re-equilibriate in the case for a non-reactive gas is just 22 h. Thus TIC re-equilibriates about 11 times more slowly than the non-reactive gas, which corresponds to a Revelle factor of about 9. This is pretty much in the middle of the range given by Broecker & Peng (1982).

Consequently, the great majority of CO_2 produced or consumed in a coastal marine ecosystem over time scales of less than a week is actually exchanged with the CO_2 in the oceanic waters and not the atmosphere. Smith (1973) pointed out that gas exchange contributed to far less than 10% of the changes observed in TIC at Enewetok Atoll, Marshall Islands. He concluded that CO_2 gas exchange can be safely ignored in calculating biological activity from changes in TIC. This is in marked contrast to the open ocean where mixing rates are strongly limited by the slow mixing of surface and deep waters and thus it is more appropriate to consider, as a first approximation, that surface waters are in equilibrium with the atmosphere.

fCO_2 gradients between coral reef and ocean waters

As gas exchange of CO_2 between sea water and the atmosphere is almost negligible on the time scales considered here, we must compare the lagoonal fCO_2 with the fCO_2 of oceanic waters flowing into the reef (Fig. 6). In October 1993, the oceanic fCO_2 was approximately atmospheric. fCO_2 at M1 is greater than the oceanic fCO_2 for over half of the time. It therefore seems that the activity in the lagoon drives a CO_2 gradient forcing

a loss of CO_2 from the system. fCO_2 at M3 reaches considerably lower values than M1 or M2, as low as 200 ppm. Due to the lack of nighttime measurements at M3, it is impossible to evaluate the source/sink behavior at the entrance of the lagoon where water flows off the reef flat, although we might conclude that the morning fCO_2 values are near the maximum due to the accumulation of CO_2 from respiratory activity over the nighttime. This would suggest that the reef is much more 'sink-like' than the lagoon and perhaps even creates a gradient of CO_2 forcing absorption to the reef system as the oceanic water flows over the reef flat.

In March 1994, the ocean fCO_2 was low, perhaps due to assimilation by spring phytoplankton blooms. This time we have complete records of fCO_2 at M1 and M2. Both of these points are characterized by water flow mainly exiting the lagoon. fCO_2 values are centered around the oceanic fCO_2, and thus on average there does not appear to be a definite fCO_2 gradient between the ocean and the reef system.

In July 1994, we have a more detailed fCO_2 profile at M3. However, we did not measure open ocean concentrations of TIC and pH at that time. We measured TIC and A_T in the waters several hundred meters offshore of the reef flat 1 mo earlier, and we have plotted this value in Fig. 6. The fCO_2 calculated from pH and TIC at M3 is generally larger than the offshore value (Fig. 6, solid line). Since the oceanic fCO_2 was calculated from TIC and A_T, we have also plotted fCO_2 values in the lagoon calculated from TIC and A_T. These values are considerably lower than the offshore value. Thus, it is impossible to draw a decisive conclusion here, although it is reasonable to suppose that the diel pattern is accurate and that the actual fCO_2 values lie somewhere between the 23 profiles.

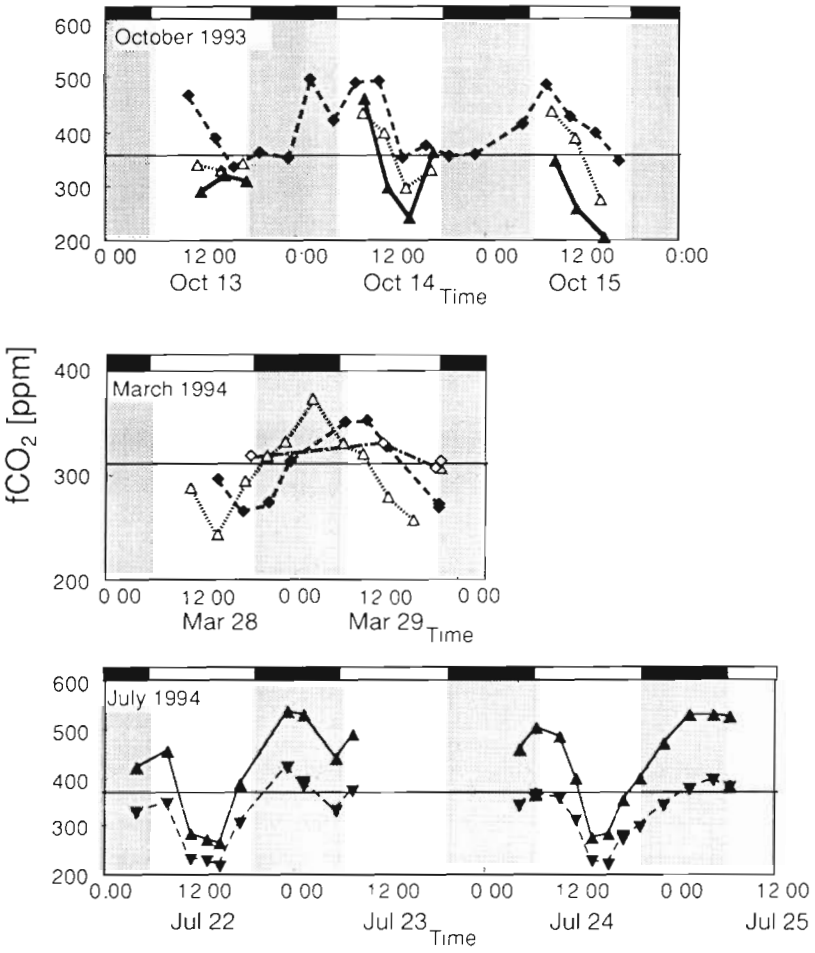

Fig. 6. Profiles of fCO_2 calculated from pH and TIC at points inside the lagoon for October 1993, March 1994 and July 1994. Profiles at M1 (—◆—), M2 (···△···), M3 (—▲—), and the observation site immediately offshore the reef flat (—◇—·) are shown. Oceanic fCO_2 is shown by the horizontal solid lines in each plot. The oceanic fCO_2s for October and March were calculated from pH and TIC. In October the oceanic fCO_2 was 360 ppm, and in March it was 308 ppm. For the July 1994 plot, the oceanic fCO_2 was calculated from TIC and A_t measurements taken from offshore waters at Miyako Island in June 1994 to be 377 ppm. Dark periods are shown by shading

Modeling production and calcification on the reef flat and in the lagoon

Frankignoulle et al. (1995) have shown that the deposition of 1 mol of $CaCO_3$ results in the release of about 0.6 mol of CO_2 under current conditions of sea water temperature and atmospheric CO_2 concentration. However, organic production fixes 1 mol of CO_2 for each mole of organic carbon produced (ignoring the minor effect of nutrient ion uptake). Thus when the ratio of organic to inorganic production is greater than 0.6, CO_2 is removed from the water column. However, while the 0.6 ratio results in no change of *in situ* CO_2, A_T is reduced with possible impacts on the biogeochemistry of the reef.

We use the alkalinity anomaly technique to determine the rate of calcification (Smith 1940). Assuming that the significant changes of A_T are mainly due to consumption of CO_3^{2-} through the precipitation and/or dissolution of calcium carbonate by living organisms, due to the double charge

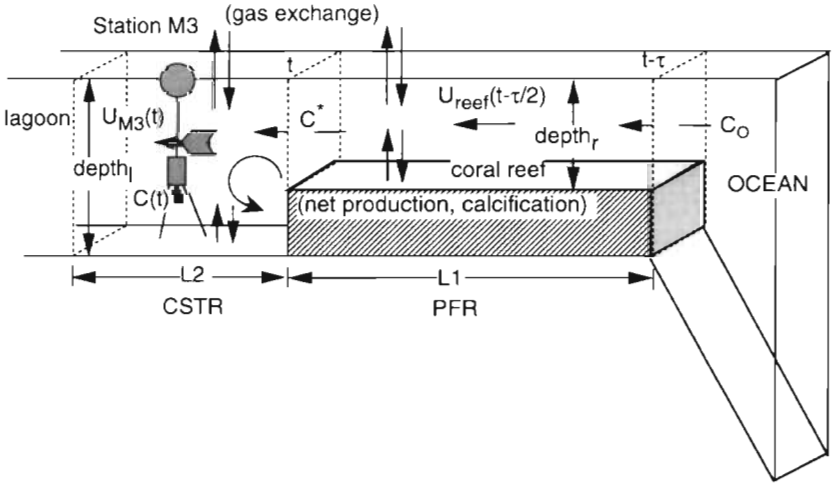

Fig. 7. Diagram of the flow model used to account for the advective supply to M3 from biological activity on the reef, modified from Kraines et al. (1996). $U_{M3}(t)$ is the measured flow speed at M3 in the direction of the primary flow where t indicates the time dependency of this variable. $U_{reef}(t)$ is the flow speed on the reef flat calculated from $U_{M3}(t)$. t is the time dependent residence time on the reef flat. C is the concentration of the modeled parameter at station M3. C^* is the concentration exiting the reef flat. C_o is the ocean concentration. $L1$ is the length of the reef flat. $L2$ is the length of the perfectly mixed region around station M3. See text for details on the model

carried by the carbonate ion, 2 mol of A_T are produced or destroyed for each mole of calcium carbonate precipitated or dissolved, respectively. Thus:

$$\text{calcification (dissolution)} = 0.5 \times dA_T/dt \ (\text{mol l}^{-1}\text{min}^{-1}) \quad (3)$$

By making some assumptions about the flow at Bora Bay, we can use the data presented above to make some preliminary estimates of gross primary production, community respiration and calcification at Bora Bay at the time of each field survey. As described by Kraines et al. (1996), the observations at M3 generally reflect the activity of the highly productive reef flat since the flow of water there is nearly always from the reef flat to the lagoon. At M1, on the other hand, observations show the integrated effect of the lagoon since the water arriving there has generally traveled through the entire lagoon.

We assume that at M3, concentrations are determined by the biological production, partially mitigated by gas exchange across the air-sea interface. The processes of production and gas exchange affect the water traveling from the ocean, across the reef and to the observation point. This formulation is equivalent to the 'plug flow reactor' (PFR) approximation employed in chemical engineering (Levenspiel 1962). As the outer oceanic concentrations of the substances which we are considering have a far smaller variance compared to concentrations within the reef system, we assume that oceanic TIC concentrations and A_T are constant for each monitoring period.

In order to calculate activity on the reef flat from observed concentrations at M3, we determine the residence time of water flowing across the reef flat as the length of the reef flat (about 300 m) divided by the flow speed on the reef flat averaged over 30 min (the average time taken for water to flow across the reef flat). The change in concentration incurred per unit area per unit time is then simply the difference of concentration between M3 and the outer ocean divided by the residence time and multiplied by the depth. However, since the M3 monitoring station is located in the lagoon and not on the reef flat, we must account for the mixing that occurs as water flows off the reef flat and into the lagoon. Fig 7 illustrates the model we have developed for this purpose.

We model the inflow of oceanic water as crossing the reef flat with length $L1$ and time dependent $depth_r$ as described above. Concentrations of TIC and A_T are altered by biological processes (we have ignored gas exchange due to the short time it takes for water to cross the reef flat in accordance to the discussion earlier). Water with the resultant time dependent concentration C^* flows into the lagoon. This water is then assumed to be perfectly mixed in a limited volume around M3 with length $L2$ and a time dependent observed $depth_l$. $L2$ is determined from continuous DO measurements (Kraines et al. 1996) as well as temperature and salinity (Kraines 1995). Finally, we compare the resulting diluted concentration with the observed concentration at M3 to derive calcification from changes in A_T and organic production from TIC. We can describe the model by the following analytical equations:

PFR flow over the reef flat:

$$C^*(t) = C_o + \frac{\tau}{depth_r(t-\tau)}\left[P^r_{net}\left(t-\frac{\tau}{2}\right)\right] \quad (4)$$

Mixed region around M3:

$$\frac{\Delta C}{\Delta t} = \frac{U_{M3}(t)}{L2}(C^*(t)-C(t)) + \frac{P^l_{net}}{depth_l(t)} \quad (5)$$

Therefore:

$$P^r_{net}\left(t-\frac{\tau}{2}\right) = \frac{depth_r(t-\tau)}{\tau}\left\{\left[\left(\frac{\Delta C}{\Delta t}\right)-\left(\frac{\Delta C_{M1}}{\Delta t}\right)\right]\frac{L2}{U_{M3}(t)} + C(t) - C_o\right\} \quad (6)$$

Here, the Cs refer to concentrations of TIC, P^{r}_{net} is net production and calcification on the reef flat, P^{l}_{net} is net production and calcification in the lagoon determined from changes observed at M1, and τ is the residence time on the reef flat calculated as described above, $depth_r$ is the depth on the reef flat and $depth_l$ the depth in the lagoon. Other notation is as shown in Fig. 7. The same equations can be used to obtain calcification from alkalinity data using the alkalinity anomaly technique. The nonsubscripted C refers to concentrations observed at M3, while C_{M1} is the concentration at station M1

We show here that at M1 the influence of reef flat waters advected to the station is of secondary importance to the production in the lagoon. Kraines et al. (1996) showed how the concentration of DO changes as water moves through the lagoon. The DO concentration entering the area where station M3 is located is sharply different from the concentration leaving that area. Therefore, the influence of advection is a dominant factor at M3. However, in the area around M1, the concentrations of DO entering and leaving are nearly the same so that the advective influence is almost negligible (see Fig. 2 in Kraines et al. 1996). The same conclusion should apply to changes in TIC and A_T.

The calculations shown above allow us to ignore the advective supply of TIC and A_T at M1. Thus at M1, we model production simply as the observed change in concentration:

$$P^{l}_{net} = \frac{\Delta C}{\Delta t} depth_l \quad (7)$$

This equation gives us an estimate for the lagoon production rate at M3 to account for the slight production and calcification occurring as water mixes off the reef flat and into the lagoon. Still, we would like to point out that the non-negligible supply of highly altered sea water from the reef flat will tend to exaggerate the concentration responses at M1 to biological activity in the lagoon though most of the reef flat production is lost when water exchanges with the ocean over the central part of the reef flat. Therefore, our calculated rates of organic and inorganic carbon production in the lagoon, both positive during the day and negative at night, may be slightly large.

Model results

Overall, both calcification and organic production show increases with light intensity with a greater light dependence of organic carbon metabolism (Fig. 8). In October, lagoon calcification ranged from an average

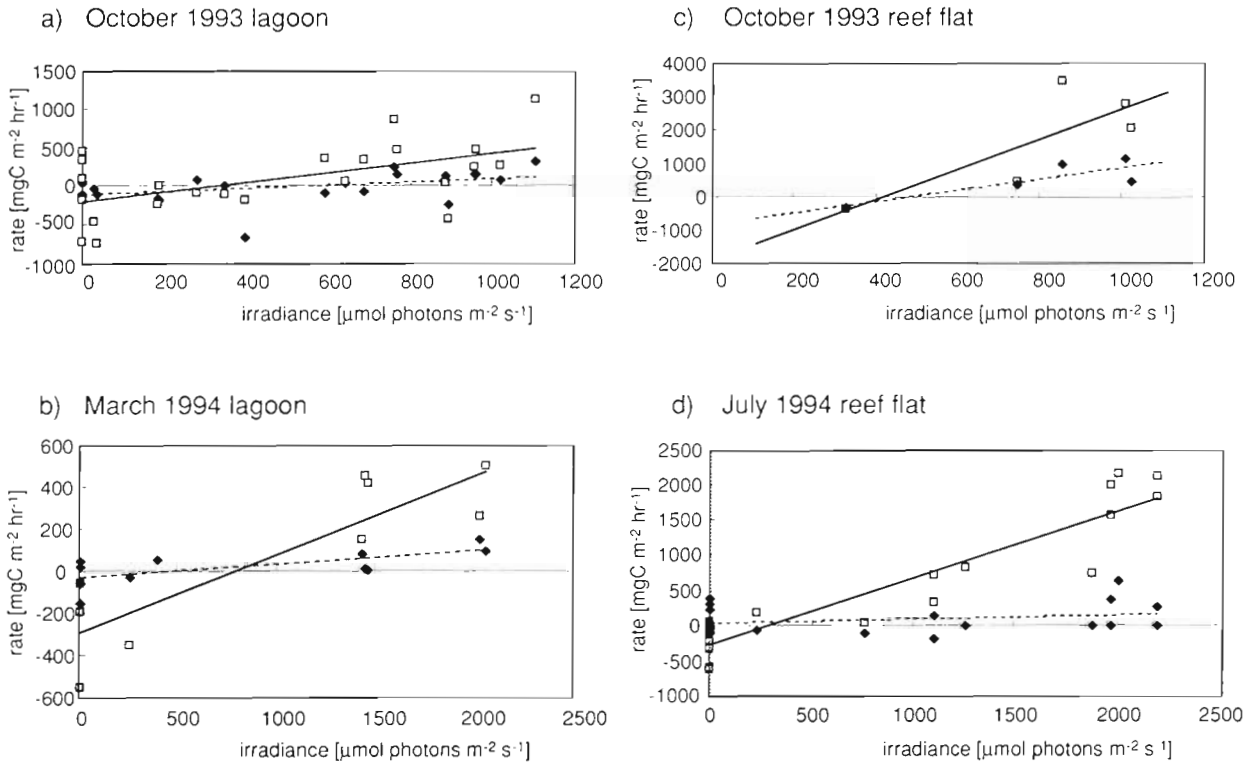

Fig. 8. Plots showing rates of organic (□) and inorganic (◆) production versus irradiance calculated for the lagoon in October (a) and March (b) and for the reef flat in October (c) and July (d) using the model described in the text and shown in Fig. 7. Linear for organic and inorganic production are shown by solid and dotted lines, respectively

of −30 mg C m^{-2} h^{-1} at low irradiance to about 200 mg C m^{-2} h^{-1} at irradiances greater than 700 µmol photons m^{-2} s^{-1}. Lagoon production ranged from an average of −170 mg C m^{-2} h^{-1} at zero irradiance to over 500 mg C m^{-2} h^{-1} at irradiances greater than 800 µmol photons m^{-2} s^{-1}. Reef flat values were much larger, from about −400 to 1000 mg C m^{-2} h^{-1} for calcification and −500 to 3000 mg C m^{-2} h^{-1} for production, though we note the lack of nighttime measurements.

In March we only have data at M1. Calcification in the lagoon calculated from this data ranges from an average of −25 mg C m^{-2} h^{-1} at zero irradiance to around 150 mg C m^{-2} h^{-1} at maximum observed irradiance, while production appears to average about −275 mg C m^{-2} h^{-1} at zero irradiance and saturate at a little over 400 mg C m^{-2} h^{-1} at an irradiance of 1600 µmol photons m^{-2} s^{-1}.

As we discussed above, the observed A_T from the July survey disagreed with the A_T calculated from pH and TIC. Therefore, we tried modeling both the observed and the calculated A_T for July. Using the observed A_T, reef flat calcification proceeded at a negative rate, i.e. dissolution occurred, for all light levels. However, when we used the calculated A_T, the calcification rates were positive at high light levels. On the reef flat, dominated by calcifying coral, negative values of calcification throughout the entire light cycle lead us to question the rates obtained from the observed A_T data. Therefore, we use the rates modeled from the calculated A_T in our discussion here. The average calcification at zero irradiance was −55 mg C m^{-2} h^{-1} and the light saturated maximum values reached up to 500 mg C m^{-2} h^{-1}. Average production at zero irradiance was −20 mg C m^{-2} h^{-1} and the maximum rate was around 2000 mg C m^{-2} h^{-1}.

We were unable to fit the calculated metabolic rates to the hyperbolic tangent light dependence formulation of Jassby & Platt (1976) due to the large scatter in the data. Therefore, we used linear regressions between the organic and inorganic production rates and light which are summarized in Table 1. The use of linear regressions is justified because the error in light measurements is much smaller than the error in the production rate estimates [see 'Results: Calculated TIC and carbonate alkalinity (A_c)']. The zero irradiance intercept corresponds to night respiration, i.e. net production when there is no light. The slope corresponds to the rate of increase in production rate with light intensity.

The calculated results for the lagoon in October and March agree fairly well, with light saturated photosynthesis (P_{sat}) at 600 to 700 mg C m^{-2} h^{-1} and night respiration equal to around −200 to −300 mg C m^{-2} h^{-1}. The night respiration values calculated as the zero intercept of the linear fit agree well with the average of the zero irradiance rates. Light saturated rates of calcification as well as zero irradiance average rates were also similar at about 150 mg C m^{-2} h^{-1} and −30 mg C m^{-2} h^{-1}, respectively. However, there is a large difference in nighttime calcification/dissolution rates calculated as the zero intercept of the linear fit in October and March. Therefore, we use the zero irradiance averages for respiration, since they are less likely to be affected by biases in the fitting approach. Net production is close to or slightly less than zero indicating a slight CO_2-source-like behavior (Table 2). Calcification overall is positive in both October and March.

The correlation of the lagoon rates with light was far better with the March data set than the October data set. This leads us to consider that the rather large negative nighttime rate of calcification calculated in October from the zero intercept may be inaccurate, with the zero irradiance average giving the better estimate. As evidenced by the better fit achieved with the more dense March data set, it should be easier to fit the hyperbolic tangent function and make better estimates of the metabolic rates with a higher frequency of measurements. Measurements should be made at least

Table 1. Summary of linear fits to organic and inorganic production rates shown in Fig. 8. The table shows average rates at zero irradiance (mg C m^{-2} h^{-1}), maximum noontime irradiance (mmol photons m^{-2} s^{-1}), slope and intercept (mg C m^{-2} h^{-1}) from the linear fits of production versus irradiance, the R^2 values of the fits, and the light saturated rate (mg C m^{-2} h^{-1}), calculated as the noon time irradiance times the slope. P: net rate of organic production (photosynthesis minus respiration); G: calcification rate

		Zero avg	Max irradiance	Slope	Intercept	R^2	Saturated rate
Oct lagoon	P	−171	1100	0.633	−206	0.31	697
	G	−29	1100	0.196	−99	0.15	216
Oct reef flat	P	-	1100	1.547	−665	0.50	1702
	G	-	1100	0.533	−162	0.49	587
Mar lagoon	P	−275	2000	0.372	−287	0.76	744
	G	−25	2000	0.064	−30	0.46	128
July reef flat	P	−54	2200	0.874	−177	0.89	1863
	G	−17	2200	0.192	−47	0.55	423

once per hour, particularly around daybreak and nightfall, in order to make best use of this model.

For the reef flat, the more complete 24 h data set taken in July gives us a fairly good correlation between irradiance and organic production. The correlation for calcification is not quite as good, but still better than in October. Note that while the saturation rates of photosynthesis and calcification in October and July are almost exactly the same, the respiration calculated from the zero intercept in October is much larger than either the linear fit or the zero irradiance average estimate for respiration in July. This difference in respiration rates results in net productions for the reef flat shown in Table 2 that are positive in July and negative in October (we have shown the respiration estimate for the October data from the zero intercept in parentheses). Calcification proceeded at a positive rate in both seasons.

In October, we only have daytime data, so the linear fit is taken from a relatively narrow range of irradiance resulting in the low correlation. Since the rates of photosynthesis are almost exactly the same in October and July, we hypothesize that the real October night respiration is considerably smaller than the value calculated from the linear fit. We omit the October 1993 reef flat R values from the following discussion.

As shown in Table 2, in July, organic production far exceeded net calcification on the reef flat, implying that the reef flat was acting in a sink-like manner in terms of CO_2 at this time of year. In October, the high rate of light saturated photosynthesis suggests that in the fall the reef flat also acts as a CO_2 sink, but we cannot make a firm conclusion due to lack of nighttime measurements as described above. In the lagoon, net production was nearly zero in October and negative, indicating a net respiration of organic material, in March as shown in Table 2. As calcification was positive overall for both periods, it appears that the lagoon, at least in the fall and spring, acts like a CO_2 source with slightly stronger source-like behavior in March (Table 2). This is supported by the high calculated fCO_2 at M1 in October shown in Fig. 6.

There has been an ongoing debate as to whether coral reefs are sinks or sources of atmospheric CO_2. Given the large number of different coral reefs in the world's oceans existing in very different environments, it is not surprising that a consensus has not been reached. Our calculations indicate that the reef flat at Bora Bay appears to be a net sink of CO_2 during the periods of our surveys. The lagoon on the other hand appears to be a net source of CO_2. However, the rates are much smaller in the lagoon than on the reef flat. Since the reef flat accounts for nearly one third of the area of the coral reef system at Bora Bay, this reef system appears to be a net sink of CO_2 overall.

Kraines et al. (1996) obtained net production rates on the reef flat and lagoon by modeling the DO profiles observed in October 1993 at Bora Bay using a tanks-in-series model for the circulation in the lagoon. Their gross production rates, shown in Table 2, are in excellent agreement with our results from an independently measured data set (TIC and A_T) using the simplified model we present here for both the reef flat and the lagoon. The respiration rates in the lagoon are also in excellent agreement; however, the respiration rate calculated by Kraines et al. (1996) for the reef flat in October is over 3 times larger than our rate for July. We cannot say now whether the difference is due to real

Table 2. Summary of metabolic rates calculated at Bora Bay. Units are g C m^{-2} d^{-1} P: gross production integrated over the light period; R: 24 h respiration. Net rates are the sums of the positive daytime rates and negative nighttime rates. Net CO_2 fixation is calculated as (net production) – 0.6(net calcification) as described in the text. The respiration estimates are all from the zero irradiance averages in Table 1 except for the October M3 estimate which is shown in parentheses

	Organic production		Calcification		Net	Net	Net
	P	R	Day	Night	production	calcification	CO_2 fixation
Bora Bay, Miyako Island; present study							
Oct 1993 lagoon	4.4	−4.1	2.2	−0.7	0.3	1.5	−0.5
Oct 1993 reef flat	10.8	(−16.0)	5.9	−3.9	(−5.1)	2.0	(−6.3)
Mar 1994 lagoon	4.2	−6.6	1.3	−0.6	−2.4	0.7	−2.8
July 1994 reef flat	14.2	−1.3	4.2	−0.4	12.9	3.8	10.6
Bora Bay, Miyako Island; Kraines et al. (1996)							
Reef flat	13.1	−5.2	–	–	7.9	–	–
Lagoon	4.9	−5.2	–	–	−0.3	–	–
Shiraho, Ishigaki Island; Nakamori et al. (1992)							
Inner coral	4.9	−4.6	2.9	−1.1	0.3	1.7	−0.7
Sand comm	0.6	−0.8	0.2	−0.3	−0.2	−0.1	−0.1
Shiraho, Ishigaki Island; Kayanne et al. (1995)							
Reef	1.8	−1.2	0.7	0.0	1.3	1.2	0.6

seasonal differences or to the difference in analytic methods. The results of Kraines et al. (1996) give a slightly more conservative net production, but even the lower net production still results in a strong net CO_2 fixation on the reef flat using our calcification rate for July. Thus it appears clear that the reef system at Bora Bay is characterized by a net CO_2 fixation on the reef flat and net CO_2 release in the lagoon with a slightly positive net fixation overall.

In one of the few systems level studies of coral reefs in the Ryukyu Islands, Nakamori et al. (1992) conducted a very comprehensive study of the current pattern and carbon fluxes at Shiraho Reef in Ishigaki Island in September 1991. They studied the biological metabolism of a sand bottom community and an inner coral community using the tent enclosure method. Net production and net calcification were 0.3 g C m^{-2} d^{-1} and 1.7 g C m^{-2} d^{-1}, respectively, for an inner reef coral community. For the sand bottom community, net production and net calcification rates were −0.2 g C m^{-2} d^{-1} and −0.1 g C m^{-2} d^{-1}, respectively. Furthermore, they used community organic and inorganic production rates from the literature to estimate productions on the reef flat for the algal reef crest community and the outer slope coral community. These values are shown in Table 2. Kayanne et al. (1995) also studied the Shiraho Reef and presented measurements of fCO_2 as well as pH and alkalinity. We have included the rates they calculated for organic and inorganic production in Table 2 as well. Overall, both reef systems appear to be characterized by net CO_2 fixation on the reef flat or reef crest, and CO_2 production in the lagoon. Nakamori et al. (1992) concluded that Shiraho exported about 8% of its gross primary production or 0.3 g C m^{-2} d^{-1} using a multiple box model.

CONCLUSIONS

We calculated the fCO_2 for each measurement period using 4 combinations of the measured parameters, and we conclude that best results were obtained from pH and TIC or pH and A_T combinations, in agreement with the observations of other researchers. Although overall the daily average fCO_2 values inside the reef system varied little from the oceanic values, there appeared to be a trend of slightly lower fCO_2 where water flows off the reef flat and into the lagoon than where the water flows out of the lagoon, indicating that the reef flat maybe slightly more sink-like than the lagoon at Bora Bay.

We attempted to quantify this with a model based on a highly simplified flow pattern. We calculated net organic and inorganic production rates as functions of light irradiance for the observation stations located where water flows off the reef flat and into the lagoon and where the water exits the lagoon. Our model is able to distinguish between flow dominated and flow negligible regimes as exemplified by the observation stations M3 and M1. The rates we have calculated agree well with the results obtained by the more sophisticated model developed by Kraines et al. (1996), showing clearly a net CO_2 fixation on the reef flat and small CO_2 release in the lagoon. However, unlike their model, the model we have presented here is able to show the dependency of the rates on irradiance. This is because, rather than specifying rates that give the best fit of modeled concentrations with observed profiles, we have calculated the rates directly from the observed data.

As each coral reef differs in its characteristics of water quality, flow patterns and community structure, the numerical rates calculated here for Bora Bay may not apply to other reefs in the Ryukyu chain, let alone reefs in other parts of the world. In addition, even at Bora Bay, production rates should vary significantly with weather conditions. However, the basic conceptual flow pattern we have described here has been observed to generally hold in coral reefs (Tait 1972, Hamner & Wolanski 1988, Wolanski et al. 1993), and we believe that the model presented here will be useful in converting point measurements to estimates of biological activity on other reef systems.

Many different varieties of reefs should be studied, including both pristine and anthropogenically influenced reefs, in order to better understand the biological and physical processes that contribute to the carbon flux as well as the ability of reefs to flush out terrestrial pollutants and so maintain healthy coral populations. The new analytical techniques and modeling procedures presented here could be valuable tools in furthering the understanding these processes where the interaction of inorganic and organic carbon productions complicate the carbon budget. From a relatively small data set, we have been able to evaluate the rates of calcification and organic carbon production. As the power of computers continues to increase, we feel that models such as the one outlined in this paper will reveal more information from limited on-site measurements.

Acknowledgements. We are deeply indebted to Richard Zimmerman, Jean-Pierre Gattuso and Atsushi Suzuki for in depth discussions regarding the material presented here. We thank Yoshinori Izuka for providing advice on the statistical analysis. We would also like to express our gratitude to Mr Hiroyuki Fujimura and Ms Satoko Nagaoka for their assistance in the analysis of pH and alkalinity. Financial support for this research was provided by the Research Institute of Innovative Technology for the Earth (RITE).

LITERATURE CITED

Atkinson MJ, Bilger RW (1992) Effects of water velocity on phosphorus uptake in coral reef-flat communities. Limnol Oceanogr 37:273–279

Ben-Yaakov S (1970) A method for calculating the in situ pH of seawater. Limnol Oceanogr 15:326–328

Bilger RW, Atkinson MJ (1995) Effects of nutrient loading on mass-transfer rates to a coral-reef community. Limnol Oceanogr 40:279–289

Broecker WS, Peng TH (1974) Gas exchange rates between air and sea. Tellus 26:21–35

Broecker WS, Peng TH (1982) Tracers in the sea. Eldigo Press, Palisades, NY

Crossland CJ, Hatcher BG, Smith SV (1991) Role of coral reefs in global ocean production. Coral Reefs 10:55–64

Dickson AG, Goyet C (1994) Handbook of methods for the analysis of the various parameters of the carbon dioxide system in sea water, Ver 2. US Dept Energy, special research grant program 89–7A: Global survey of carbon dioxide in the oceans

Frankignoulle M, Pichon M, Gattuso JP (1995) Aquatic calcification as a source of carbon dioxide. In: Beran MA (ed) Carbon sequestration in the biosphere. NATO ASI Series Vol I 33. Springer-Verlag, Berlin, p 265–271

Gattuso JP, Pichon M, Delesalle B, Frankignoulle M (1993) Community metabolism and air-sea CO_2 fluxes in a coral reef ecosystem (Moorea, French Polynesia). Mar Ecol Prog Ser 96:259–267

Hamner WM, Wolanski E (1988) Hydrodynamic forcing functions and biological processes on coral reefs: a status review. Proc 6th Int Coral Reef Symp 1:103–113

Hearn CJ, Parker IN (1988) Hydrodynamic processes on the Ningaloo coral reef, western Australia. Proc 6th Int Coral Reef Symp 2:497–502

Ikeda Y, Suzuki A, Hata H, Kato K, Negishi A, Nozaki K (1995) Closed chamber system for estimating rate of carbon production by coral reef organisms. J Mar Biotechnol 2:119–123

Jassby AD, Platt T (1976) Mathematical formulation of the relationship between photosynthesis and light for phytoplankton. Limnol Oceanogr 21:540–547

Johansson A, Wedborg M (1982) On the evaluation of the potentiometric titrations of the seawater with hydrochloric acid. Oceanol Acta 5:209–218

Johnson KM, Sieburth JMcN, Williams PJLeB, Brändström L (1987) Coulometric total carbon dioxide analysis for marine studies: automation and calibration. Mar Chem 21: 117–133

Kayanne H, Suzuki A, Sato H (1995) Diurnal changes in the partial pressure of carbon dioxide in coral reef water. Science 269:214–216

Kinsey DW (1985) Metabolism, calcification and carbon production I: Systems level studies. Proc 5th Int Coral Reef Congr 4:505–526

Kinsey DW, Hopley D (1991) The significance of coral reefs as global carbon sinks—response to greenhouse. Palaeogeogr Palaeoclimatol Palaeoecol 89:363–377

Kirk JTO (1983) Light and photosynthesis in aquatic ecosystems. Cambridge University Press, Cambridge

Kraines SB (1995) Construction of a model of mass flux in a coral reef. Master's thesis, University of Tokyo

Kraines SB, Suzuki Y, Yamada K, Komiyama H (1996) Separating biological and physical changes in dissolved oxygen concentration in a coral reef. Limnol Oceanogr 41: 1790–1799

Levenspiel O (1962) Chemical reaction engineering. Wiley, New York

Lewis JB (1977) Processes of organic production on coral reefs. Biol Rev 52:305–347

Mehrbach C, Culberson CH, Hawley JE, Pytkowicz RM (1973) Measurement of the apparent dissociation constants of carbonic acid in seawater at atmospheric pressure. Limnol Oceanogr 18:897–907

Millero FJ (1995) Thermodynamics of the carbon dioxide system in the oceans. Geochim Cosmochim Acta 59:661–677

Millero FJ, Byrne RH, Wanninkhof R, Feely R, Clayton T, Murphy P, Lamb MF (1993) The internal consistency of CO_2 measurements in the equatorial Pacific. Mar Chem 44:269–280

Nakamori T, Suzuki A, Iryu Y (1992) Water circulation and carbon flux on Shiraho coral reef of the Ryukyu Islands, Japan. Cont Shelf Res 12:951–970

Parnell KE (1988) The hydrodynamics of fringing reef bays in the great barrier reef marine park. Proc 6th Int Coral Reef Symp 2:503–508

Smith CL (1940) The Great Bahama Bank. II. Calcium carbonate precipitation. J Mar Res 3:171–189

Smith SV (1973) Carbon dioxide dynamics: a record of organic carbon production, respiration, and calcification in the Eniwetok reef flat community. Limnol Oceanogr 18: 106–120

Smith SV (1984) Phosphorus versus nitrogen limitation in the marine environment. Limnol Oceanogr 29:1149–1160

Smith SV (1985) Physical, chemical and biological characteristics of CO_2 gas flux across the air-water interface. Plant, Cell Environ 8:387–398

Smith SV, Veeh HH (1989) Mass balance of biogeochemically active materials (C, N, P) in a hypersaline gulf. Estuar Coast Shelf Sci 29:195–215

Suzuki A, Nakamori T, Kayanne H (1995) The mechanism of production enhancement in coral reef carbonate systems: model and empirical results. Sediment Geol 99:259–280

Tait RJ (1972) Wave set-up on coral reefs. J Geophys Res 77: 2207–2211

Wanninkhof R (1992) Relationship between wind speed and gas exchange over the ocean. J Geophys Res 97: 7373–7382

Wolanski E, Delesalle B, Dufour V, Aubanel A (1993) Modeling the fate of pollutants in the Tiahura Lagoon, Moorea, French Polynesia. 11th Australasian Conference on Coastal and Ocean Engineering, p 583–589

Zimmerman RC, Coyer JA, Steller DL, Alberte RS (1993) Algal distribution and productivity in coral ship lagoon, Miyako Jima, Japan. A data report for the Coral Ship Project

This article was submitted to the editor

Manuscript received: December 2, 1996
Revised version accepted: June 17, 1996